

The structural stability and electrical properties of $\text{Sr}_2\text{FeMo}_x\text{Nb}_{1-x}\text{O}_6$ ($x = 0, 0.3$) under high pressure

X Zhao^{1,2}, R C Yu^{1,4}, L D Yao¹, F Y Li¹, Z X Liu¹, Z X Bao¹, X D Li³,
Y C Li³, M N Ma³, J Liu³, G D Tang² and C Q Jin¹

¹ Key Laboratory of Extreme Conditions Physics, Institute of Physics, Centre for Condensed Matter Physics, Beijing High Pressure Research Centre, Chinese Academy of Sciences, PO Box 603, Beijing 100080, People's Republic of China

² Department of Physics, Hebei Normal University, Shijiazhuang 050016, Hebei, People's Republic of China

³ Institute of High Energy Physics, Chinese Academy of Sciences, Beijing 100039, People's Republic of China

Received 25 August 2003

Published 13 February 2004

Online at stacks.iop.org/JPhysCM/16/1299 (DOI: 10.1088/0953-8984/16/8/014)

Abstract

The resistance–pressure (R – P) and capacitance–pressure (C – P) relationships for the compounds $\text{Sr}_2\text{FeMo}_x\text{Nb}_{1-x}\text{O}_6$ ($x = 0, 0.3$) have been studied in the pressure range of 0–20 GPa using a diamond anvil cell at room temperature. According to the analysis of energy dispersive x-ray diffraction with synchrotron radiation, in the range of experimental precision, the changes in R – P and C – P for $\text{Sr}_2\text{FeNbO}_6$ and $\text{Sr}_2\text{FeMo}_{0.3}\text{Nb}_{0.7}\text{O}_6$ at about 7.5 and 2.8 GPa, respectively, are considered as electronic transitions caused by high pressure.

1. Introduction

Tunnelling-type magnetoresistance (TMR) across the grain boundaries in polycrystalline ceramics of perovskite-type transition metal oxide has been recently investigated extensively [1–3]. In this sense, oxides with both high spin polarization and high Curie temperatures are desirable. Kobayashi *et al* [4] have reported a high spin polarization for an oxide compound with an ordered double-perovskite structure, $\text{Sr}_2\text{FeMoO}_6$, which shows the colossal magnetoresistance effect at room temperature. Its high Curie temperature, $T_c \approx 420$ K, makes it a promising candidate to work at room temperature. In order to explore other prospective compounds of the same family that could be useful for this purpose, we have investigated the structural and magnetic properties of $\text{Sr}_2\text{FeMo}_x\text{Nb}_{1-x}\text{O}_6$ bulk polycrystals. The details of some of their properties will be described elsewhere [5].

$\text{Sr}_2\text{FeMoO}_6$ is known as a ferromagnetic metal [4], where Fe^{3+} ($S = 5/2$) and Mo^{5+} ($S = 1/2$) couple antiferromagnetically. In $\text{Sr}_2\text{FeMoO}_6$, the $3d^5$ electrons of Fe^{3+} ions are

⁴ Corresponding author.

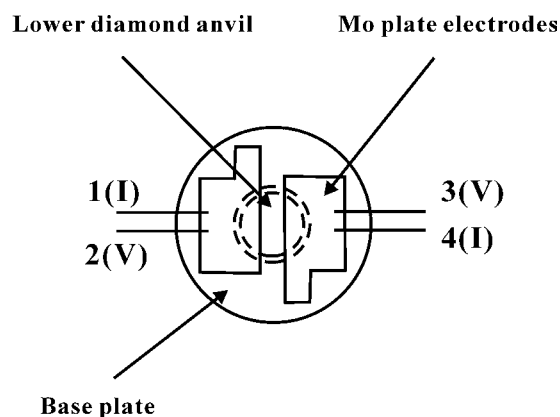


Figure 1. Top view of Mo electrodes placed on the lower diamond anvil.

considered as localized, showing local spin moment $S = 5/2$, while the $4d^1$ electrons of Mo^{5+} occupy the conduction band, showing spin moment $S = 1/2$ along the opposite direction. However, $\text{Sr}_2\text{FeNbO}_6$ is an antiferromagnetic insulator with T_N of 25 K, where the magnetic moments of Fe^{3+} ions show antiferromagnetic interactions at low temperature [6]. The electrical resistance shows an electronic structural transition at about 2.1 GPa in $\text{Sr}_2\text{FeMoO}_6$ under high pressure [7]. Since internal chemical pressure will be produced by the substitution of Nb for Mo, it is meaningful to study the structural stability and electrical properties in these compounds under external pressures. This will be helpful for further understanding the CMR effect in double-perovskite compounds. In this paper, we address ourselves to study the structural stability and electrical properties under high pressures in two samples of $\text{Sr}_2\text{FeNbO}_6$ and $\text{Sr}_2\text{FeMo}_{0.3}\text{Nb}_{0.7}\text{O}_6$.

2. Experiments

The polycrystalline samples of the compounds $\text{Sr}_2\text{FeNbO}_6$ and $\text{Sr}_2\text{FeMo}_{0.3}\text{Nb}_{0.7}\text{O}_6$ were prepared by using a traditional solid-state reaction method. Stoichiometric mixtures of SrCO_3 , Fe_2O_3 , MoO_3 , and Nb_2O_5 were first calcined at 1000°C for 4 h in a flow of Ar gas, and then mixed thoroughly in an agate mortar and pressed into pellets. The pellets were sintered at 1100°C for 3 h in a 1% H_2/Ar flow, and finally at a temperature of 1125°C for 16 h with several intermediate grindings.

The *in situ* high-pressure x-ray energy dispersive diffraction experiments on $\text{Sr}_2\text{FeNbO}_6$ and $\text{Sr}_2\text{FeMo}_{0.3}\text{Nb}_{0.7}\text{O}_6$ were carried out with a diamond anvil cell (DAC) at room temperature at the Beijing Synchrotron Radiation Facility (BSRF). The size of the x-ray spot was $120\ \mu\text{m} \times 120\ \mu\text{m}$ and the culet of the DAC was $500\ \mu\text{m}$. The sample powder was loaded with the inner pressure standard Pt powder into a $300\ \mu\text{m}$ hole in a T301 stainless steel gasket. The pressure in the DAC was calculated according to the equation of state of Pt [8]. In our experiments, the relation between energy and channel was $E = 0.48611 + 0.0082 \times \text{chn}$. The diffraction angles used for $\text{Sr}_2\text{FeNbO}_6$ and $\text{Sr}_2\text{FeMo}_{0.3}\text{Nb}_{0.7}\text{O}_6$ in the experiments were 9.2322° and 9.2538° , respectively.

The changes of resistance (R) and capacitance (C) of the samples with pressure were measured simultaneously in a DAC with a ZL5 intelligent inductance–capacitance–resistance (LCR) meter at 1 kHz. The techniques used for the DAC and measurements were the same as those used previously [9]. Figure 1 shows a schematic diagram of the molybdenum electrodes

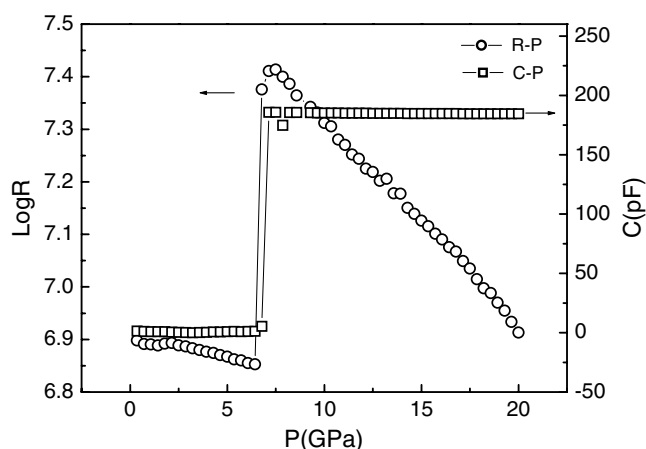


Figure 2. R - P and C - P relationships of $\text{Sr}_2\text{FeNbO}_6$.

placed on the lower diamond anvil. Two parallel Mo sheets were used as electrodes of a capacitor as well as the probes in resistance measurements. There are two leads for each electrode, and one of the two leads is used for the current and the other for voltage (1, 4 and 2, 3 are used for current and voltage, respectively). The Mo electrodes were made by photoetching them away from a base, which was a phenolic methylal glue film with a thickness of 0.04 mm. The electrode thickness is 0.008–0.010 mm, while the distance between the two electrodes is 0.03–0.05 mm. From these dimensions, it is evident that the device is far from ideal parallel-plate capacitor geometry, but it has the capability of detecting capacitance changes associated with phase transitions. The LCR meter calculates and gives the R and C values simultaneously according to the current and voltage in the experiments. All the samples studied were pre-pressed under 2.9 GPa to make a compact sample before the measurement. Here we should point out that the resistance/capacitance and energy dispersive x-ray diffraction measurements are separate ones.

3. Results and discussion

The structure of the prepared samples was checked by x-ray powder diffraction and both samples show the orthorhombic structure. No trace of impurities was detected in the measurement. The compositions of the samples, checked by energy dispersive x-ray microanalysis *in situ* with a scanning electron microscope, are very close to the nominal ones, showing the single phase of the samples.

The open circles in figure 2 present the pressure dependence of the resistance of $\text{Sr}_2\text{FeNbO}_6$ at room temperature. In the pressure range of $0 \leq P \leq 6.4$ GPa, the resistance of the sample reduces gradually with increasing pressure, which shows the further compaction of the sample. With further increasing pressure, the resistance enhances steeply in the range of $6.4 \leq P \leq 7.5$ GPa, and decreases slowly up to 20 GPa, showing a maximum at about 7.5 GPa. The capacitance versus pressure was also measured simultaneously for the sample and the result is also shown in figure 2 with open squares. With increasing pressure, the capacitance also rises abruptly at about 7.5 GPa from a constant value of about 1.20–185.71 pF and then almost keeps the same value with further increase of pressure. As to the consistent sharp changes in resistance and capacitance at about 7.5 GPa, we think that they may be induced by either a crystal structure or an electronic structure transition.

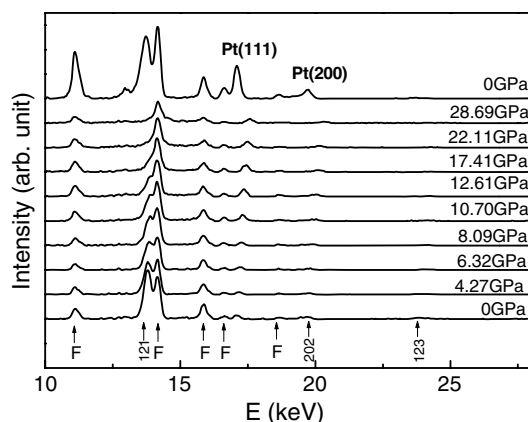


Figure 3. Energy dispersive x-ray diffraction patterns of $\text{Sr}_2\text{FeNbO}_6$ at different pressures.

In order to distinguish the transition type, the crystal structure stability of $\text{Sr}_2\text{FeNbO}_6$ under high pressure has been checked by the energy dispersive x-ray diffraction with a DAC at different pressures. The diffraction patterns are shown in figure 3. The ambient-pressure diffraction pattern shows two Pt peaks and three sample peaks, (121), (202) and (123). Several fluorescence peaks of the sample elements occur in the patterns and they are marked as 'F'. The positions of F peaks do not shift with changing pressure in the experiments since the pressure we used is too small to change the state of shells or sub-shells of the elements. Due to the presentation of all the diffraction patterns in one figure, the figure resolution for the naked eye is reduced. Though the 202 peak of the sample is near the 200 peak of Pt, the resolution is high enough in each amplified pattern to read out the position value. The maximum pressure applied is 28.69 GPa. From figure 3, it can be seen that no changes occur except a slight shift of the sample peaks in the patterns with increasing pressure. When pressure is released to the ambient, all the sample peaks come back to the original sites. The weakening of the sample peak intensity at high pressures is due to the sample flow out of the sample hole, and slight broadening of the peaks is caused by the sample thinning and pressure gradients in the sample at high pressures. This indicates that in the range of experimental precision no crystal structural transition was observed in the measured pressure range except some crystal compression under high pressure, which suggests that the crystal structure of $\text{Sr}_2\text{FeNbO}_6$ is stable in the pressure range of 0–28.69 GPa. According to the analysis of the energy dispersive x-ray diffraction results, the remarkable change in the resistance and capacitance at about 7.5 GPa can be considered as an electronic structural transition.

The R – P and C – P relationships for $\text{Sr}_2\text{FeMo}_{0.3}\text{Nb}_{0.7}\text{O}_6$ at room temperature are plotted with open circles and squares, respectively, in figure 4. As shown in figure 4, the resistance of the sample remains nearly a constant at first and then drops steeply in the range of $2.5 \leq P \leq 3.2$ GPa, and levels off up to 20 GPa. With increasing pressure, the simultaneously measured capacitance holds the line at first and then rises abruptly in the range of $2.8 \leq P \leq 3.2$ GPa. The changes in resistance and capacitance suggest either a crystal structural transition or an electronic structural transition.

Figure 5 presents the energy dispersive x-ray diffraction patterns of $\text{Sr}_2\text{FeMo}_{0.3}\text{Nb}_{0.7}\text{O}_6$ at different pressures. The maximum pressure applied is 32.4 GPa. Similar to the case of $\text{Sr}_2\text{FeNbO}_6$, no crystal structural change was observed in the measured pressure range. So the change in the resistance and capacitance at about 2.8 GPa is also induced by an electronic structural transition.

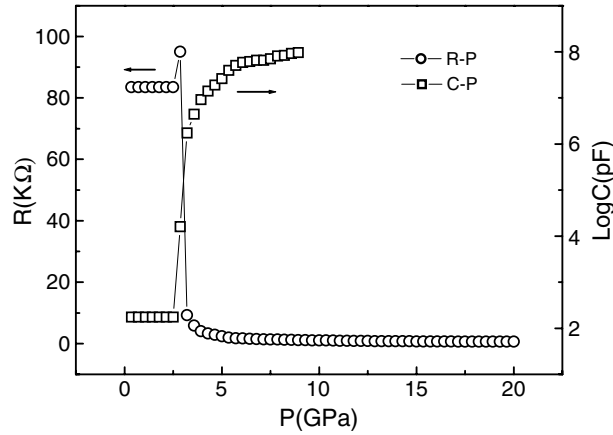


Figure 4. R - P and C - P relationships of $\text{Sr}_2\text{FeMo}_{0.3}\text{Nb}_{0.7}\text{O}_6$.

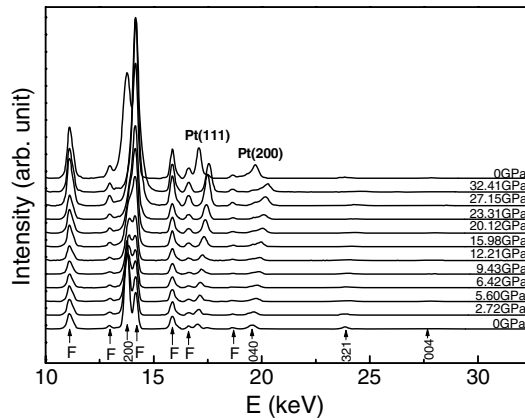


Figure 5. Energy dispersive x-ray diffraction patterns of $\text{Sr}_2\text{FeMo}_{0.3}\text{Nb}_{0.7}\text{O}_6$ at different pressures.

The change of the compressibility under high pressure sometimes gives the relevant information of electronic and structural transitions. Tang *et al* [10] investigated the pressure-induced valence state of the Tm ions in TmTe by x-ray diffraction and magnetic susceptibility. Figure 6(a) shows the V/V_0 - P curve for $\text{Sr}_2\text{FeMo}_{0.3}\text{Nb}_{0.7}\text{O}_6$ in the pressure range of 0–32.4 GPa, from which one can see that the volume of the unit cell decreases with increasing pressure. The experimental data are fitted by the Birch–Murnaghan (BM) equation:

$$P = \frac{3}{2}B_0 \left[\left(\frac{V}{V_0} \right)^{-\frac{7}{3}} - \left(\frac{V}{V_0} \right)^{-\frac{5}{3}} \right] \left\{ 1 - \frac{3}{4}(4 - B'_0) \left[\left(\frac{V}{V_0} \right)^{-\frac{2}{3}} - 1 \right] \right\}.$$

The bulk modulus B_0 and its first-order derivative B'_0 for $\text{Sr}_2\text{FeMo}_{0.3}\text{Nb}_{0.7}\text{O}_6$ are obtained to be $B_0 = 300.2 \pm 6.6$ GPa and $B'_0 = 4$.

From figure 6(a) we can see that the volume decreases continuously with increasing pressure, showing no crystal structural transition in the measured pressure range. The second experimental point in figure 6(a) seems to fall off the fitted curve. In order to make clear the behaviour of volume change in the lower pressure range, we carried out another experiment to measure the P - V relationship using a piston–cylinder type measurement device [11]. This

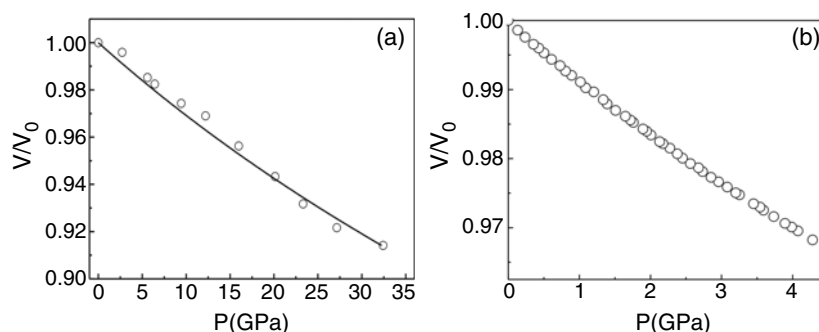


Figure 6. (a) The V/V_0 - P curve for $\text{Sr}_2\text{FeMo}_{0.3}\text{Nb}_{0.7}\text{O}_6$. Open circles represent the experimental data and the solid line represents the fitted curve. (b) V/V_0 - P data for $\text{Sr}_2\text{FeMo}_{0.3}\text{Nb}_{0.7}\text{O}_6$ in the pressure range of 0–4.5 GPa obtained using a piston–cylinder type measurement device.

device can be used only in the lower pressure range. Figure 6(b) presents the V/V_0 - P data measured by this method where no anomaly is observed. The slight falling off of the second experimental point in figure 6(a) may be caused by a slight change of the centre of the focused x-ray beam in the sample during the sample thinning at the beginning of the loading pressure. This will give rise to a small change in diffraction angle, further to the calculated d values. The V/V_0 - P curve for $\text{Sr}_2\text{FeNbO}_6$ is left out since $\text{Sr}_2\text{FeNbO}_6$ shows similar compressibility behaviour to $\text{Sr}_2\text{FeMo}_{0.3}\text{Nb}_{0.7}\text{O}_6$.

No crystal structural transition has been observed in the two compounds in the measured pressure range. This is in accord with the stability of the perovskite-like oxides under high pressure. However, the experimental results show that the electronic structure of these compounds is not stable in the measured pressure range. The electronic structural transition may be caused by the compression of the unit cell, which results in changes of band structures. It is interesting that the electronic structural transition occurs at different pressures in the two compounds. The possible scenarios to explain the difference are that the unit cell, bond distances, bond angles and related band structures are changed by the substitution of Nb for Mo.

4. Conclusions

The crystal structural stability and electrical properties of $\text{Sr}_2\text{FeNbO}_6$ and $\text{Sr}_2\text{FeMo}_{0.3}\text{Nb}_{0.7}\text{O}_6$ under high pressure have been studied using energy dispersive x-ray diffraction with synchrotron radiation and resistance and capacitance measurements, respectively, at room temperature. The energy dispersive x-ray diffraction results show that the crystal structure of $\text{Sr}_2\text{FeNbO}_6$ and $\text{Sr}_2\text{FeMo}_{0.3}\text{Nb}_{0.7}\text{O}_6$ remains stable up to 28.7 and 32.4 GPa, respectively. However, an electronic structural transition occurs in both of the samples at about 7.5 and 2.8 GPa, respectively.

Acknowledgments

This work was supported by the National Natural Science Foundation of China (No 10274099) and the State Key Development Project on Fundamental Research (No 2002CB613301).

References

- [1] Sun J Z, Gallagher W J, Dumcombe P R, Elbaum L K, Altman R A, Gupta A, Lu Y, Gong G Q and Xiao G 1996 *Appl. Phys. Lett.* **69** 3266
- [2] Lu Y, Li X W, Gong G Q, Xiao G, Gupta A, Lecoeur P, Sun J Z, Wang Y Y and Dravid V P 1996 *Phys. Rev. B* **54** R8357
- [3] Hwang H Y, Cheong S W, Ong N P and Batlogg B 1996 *Phys. Rev. Lett.* **77** 2041
- [4] Kobayashi K-I, Kimura T, Sawada H, Terakura K and Tokura Y 1998 *Nature* **395** 677
- [5] Zhao X, Yu R C, Li F Y, Liu Z X, Tang G D and Jin C Q 2004 to be submitted
- [6] Tezuka K, Henmi K and Hinatsu Y 2000 *J. Solid State Chem.* **154** 591
- [7] Zhao P, Yu R C, Li F Y, Liu Z X, Jin M Z and Jin C Q 2002 *J. Appl. Phys.* **92** 1942
- [8] Holmes N C, Moriarty J A, Gathers G R and Nellis W J 1989 *J. Appl. Phys.* **66** 2962
- [9] Bao Z X, Schmidt V H and Howell F L 1991 *J. Appl. Phys.* **70** 6804
- [10] Tang J, Kosaka T, Matsumura T, Matsumoto T, Mori N and Suzuki T 1996 *Solid State Commun.* **100** 571
- [11] Bao Z X, Gu H C and Zhang Z T 1987 *Chin. J. High Pressure Phys.* **1** 188